

Enhancing the Thermal Performance of a Double Pipe Heat Exchanger in Turbulent Flow Conditions

Manish Sanserwal^{1,2}, Devendra Yadav^{1*}, and Mayank Bhardwaj³, Gurjeet Singh⁴

¹Department of Mechanical Engineering, Galgotias College of Engineering and Technology, Greater Noida 201308, Uttar Pradesh, India

²Department of Mechanical Engineering, Delhi Technological University, Delhi, India

³University Institute of Engineering and Technology, Kurukshetra University, Kurukshetra, Haryana, India

⁴Department of Mechanical Engineering, PEC University of Technology, Chandigarh, India
E-mail: ^{1*}ydevendra393@gmail.com

Received 4 February 2022, Revised 13 April 2022, Accepted 27 April 2022

Abstract

Heat exchangers with high thermal performance are required for industrial applications. Using heat transfer methodology in conjunction with simple design changes and assembly functions of heat exchangers could be an effective way to accomplish this. An experimental analysis was performed in this study to improve the heat transfer performance of a double pipe heat exchanger by implanting a flat strip spring turbulator (FST) within the heat exchanger's inner tube. The experimental investigation of the Double pipe heat exchanger in conjunction with three sets of FST turbulators (pitch: 15 cm, 10 cm, and 5 cm) for turbulent flow (Re 9000-38000) was carried out. The Nusselt number, friction factor ratio, and thermal performance factor of heat exchangers with FST at various pitches are found to be between 60 and 170, 1.44 and 1.76, and 0.94 and 1.06, respectively. The highest heat transfer achieved by using a flat spring turbulator is 20% for a pitch value of 5cm. In comparison to other sets of FST, a double pipe heat exchanger with FST pitch value of 10 cm has greater thermohydraulic performance. When compared to previous research, the experimental results obtained from this work at higher Reynolds numbers the friction factor are within a well-accepted range.

Keywords: Heat exchanger; spring turbulator; thermal performance factor; heat transfer coefficient; Wilson plot.

1. Introduction

The heat exchanger allows heat to be transferred from the hotter fluid to the cooler fluid. There are essentially two types of categories: direct and indirect. In comparison to direct heat exchangers, indirect heat exchangers are more commonly used in industries since they eliminate fluid mixing during operation. In the current context, designing a heat exchanger is not an easy task because it still has scale and fluid flow rate constraints depending on the application. To obtain high heat transferability in heat exchangers, more attention on size reduction is required. The numerous techniques used in the heat exchanger to improve the rate of heat transfer [1]–[4], can be categorized as active, passive, and combined techniques (Fig. 1). Mechanical aids, injection, suction, electrostatic fields, and surface and fluid vibration all demand more power (external power) than the power used to run the heat exchanger. In contrast, in passive approaches, specially engineered geometries or turbulent circulation generators or turbulators are employed to impede the fluid flow with the purpose of enhancing heat transfer without the use of an external (additional) power source [5]. Multiple heat transfer improvement approaches, such as the use of twisted strips and tapes, coil or helical wire, polished surfaces, rough surfaces, stretched surfaces, perforated conical rings, conical springs, and so on, are included in the passive approach. However, the compound strategy combines passive and active methods to improve the thermo-

hydraulic performance of a heat exchanger. Hence, heat transfer enhancement in a heat exchanger can also be procured by creating turbulence in the fluid flow and at last, considering this concept as a motivation for literature. Therefore, the literature study was carried out to investigate how much higher the heat transfer rate in the heat exchanger with turbulators can be achieved. For the improvement in heat transfer rate with a full width twisted tape under laminar flow and steady wall temperature condition, Dasmahapatra & Rao [6] utilizes a viscous non-Newtonian fluid. Al-Fahed & Chakroun [7] experimentally investigated the heat transfer enhancement in a fully developed turbulent flow with a tube-tape clearance under constant heat flux condition. Whereas, an experimental study on twisted tape turbulator in a horizontal tube under viscous flow conditions were carried out by Manglik & Bergles [8]. Zamankhan [9] studied an improvement in the heat transfer rate in a heat exchanger with a helical metal wire turbulator using a glycol-water solution as a working fluid with varying concentrations. The 3D mathematical model, also developed for the confirmation of experimental data and the comparison of numerical findings with experimental results, concluded that actual system behaviors could be predicted by the LES model. [10] investigate conical spring turbulators in different configurations (convergent, divergent, and convergent-divergent conical rings CR, DR, and CDR) at different cone angles of 30°, 45°, 60° in a concentric double pipe heat

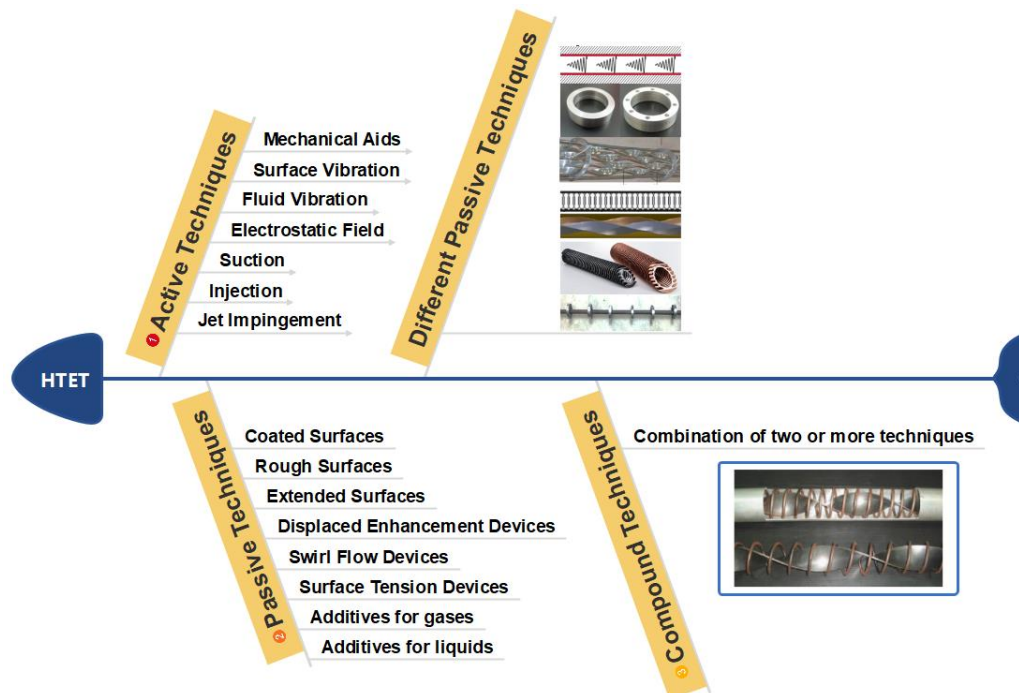


Figure 1. Techniques for heat transfer enhancement (HTET).

exchanger at different Reynolds number (10000-34000). Yadav et al. [11], [12] designed and fabricated a trio tube heat exchanger setup which has the better heat transfer capability and also compact in size. This heat exchanger requires $\approx 58\%$ smaller in pipe length for the same amount of heat transfer as of double pipe heat exchanger. Sheikholeslami et al. [13]–[15] conducted an experimental investigation on a double pipe air to water heat exchanger with discontinuous helical turbulators (typical plane and perforated) at different Reynolds numbers, pitch and open area ratio for estimating the behaviour of heat transfer and pressure drop. For finding the optimal design of heat exchanger, Non-dominated Sorting Genetic Algorithm II (NSGA II) is used for having high efficiency and ANSYS FLUENT14 for better numerical simulation.

Later on, in the same scenario, the investigation was conducted typical and perforated circular-ring (TCR and PCR) turbulators. Nanan et al. [16] carried out a comparative investigation in a heat exchanger between different turbulators designs: twisted and straight cross-baffles, twisted-baffles, alternate twisted and straight alternate-baffles and last one is straight baffles and with different pitch ratios ($P/D = 1$ to 2) and Reynolds number (6000 to 20000). For better comparison, a numerical simulation also is done with all types of turbulator for a better understanding of heat transfer enhancement and friction factor. Mashoofi et al. [17] investigated tube in tube helically coil (TTHC) heat exchange with and without helical wire turbulator in four ways: TTHC heat exchanger a) with turbulator inside the inner tube b) with turbulator inside the annulus c) with turbulator inside both tube d) without turbulator, for evaluating the effect on heat transfer and frictional factor. The use of turbulator only in the annulus (containing hot water) and turbulator only in an inner tube (containing air) enhance the airside Nusselt number by 8-32% and 52-82%, respectively. Later, a helical wire turbulator (only inside the tube) in the shell and tube helically coiled heat exchanger was investigated by Panahi et al. [18]. Sandeep et al. [19] experimentally and numerically investigated a novel turbulator (aluminum small plate placed in the cross-type

arrangement) act as airflow divider at a different pitch to tube diameter ratios varying from 0.54 to 1.09 at a 90° angle of twist. For evaluating the Nusselt number enhancement at a different angle of twist (45° and 30°), a CFD simulation was conducted and find out 1.33 to 1.46 times and 1.43 to 1.60 times of enhancement at 45° and 30° , respectively. Khorasani et al. [20] investigated the effect of a spiral wire turbulator with four different-different spring pitches and wire diameter in a helical tube with constant heat flux. Further, each arrangement was conducted for five types of flow rates of water. It is found that, with the increase in spring pitch and wire diameter of the spiral wire turbulator, Nusselt number also increases up to 70% and 73% respectively. Zohiret. al. [21] utilize a coiled wire turbulator upon the outer surface of the inner tube of double pipe heat exchanger and achieve convective heat transfer coefficient enhancement of 400% and 450% in parallel (same direction) and counterflow (opposite direction) respectively. Budaket. al. [22] numerically analyzes the four geometries of turbulators in concentric pipe heat exchanger located inside the inner pipe and considering both parallel flow and counter flow condition at different flow rates. Also, formed an ANSYS 12.0 fluent program code to analyses pressure and thermal characteristics. Kumar et. al. [23] included the effect of perforation index ($PI = 8\%$ to 24%) and found, 4 and 1.47 times of heat transfer enhancement at $PI=8\%$ & $d/D=0.6$ and $PI=24\%$ & $d/D=0.8$ condition, respectively when compared with the plain tube. Singh et. al. [24] experimentally investigated circular solid ring turbulator with multiple twisted tape arrangements inside the core. Later, Kumar et al.[25] utilized both solid and perforated circular-ring turbulator with twisted tape for investigation. Results revealed improvement in both, heat transfer and thermal performance factor over the smooth pipe in a range of around 2.2-3.54 and 1.18- 1.64 times, respectively. Whereas, Dattet. al. [26] investigated a solid circular ring turbulator with a number (ranges 1 to 4) of square wing twisted tape. Akpinar [27] experimentally studied the effect of helical spring turbulator inside the inner pipe of a double pipe heat exchanger on heat transfer and friction factor. Nusselt

number and dimensionless exergy loss increment found to be 2.64 and 1.16 times, respectively as compared to the heat exchanger not using turbulator. Maradiya et. al. [28] revealed that twisted tape as turbulator not performed well with air as compare to water as a working fluid due to large density of liquid. Also, in case of air heating application, ribs or deflector and vortex generators, whereas, in case of liquids, swirl producing devices are more useful in thermal performance factor improvement.

According to the literature and recent review papers [29]–[31], passive turbulators perform better in the water medium than in the air medium in the double concentric pipe heat exchanger. In most cases, turbulators clearly increase the heat transfer rate to a significant level at a high Reynolds number. The majority of the researches concentrated on disturbing the fluid not only in the centre but also along the wall of the heat exchanger tube (where turbulators are inserted) in order to disturb the laminar sub-layer. The current study used a flat strip spring turbulator (FST) to alleviate the disadvantages associated with earlier investigations, namely the higher value of the friction factor. This FST design advantage of less material use and to expect the maximum possible increase in heat transfer at the lowest pressure drop. So far, no experimental work on flat metal strip springs has been published; this is a novel design consisting of circular rings, springs, and twisted tape to provide better distribution of fluid streams with lower frictional loss. This research also focuses on the employment of several sets of FST turbulator to obtain the best FST value for maximum thermohydraulic performance.

2. Experimental

2.1 Fabrication of Experimental Setup

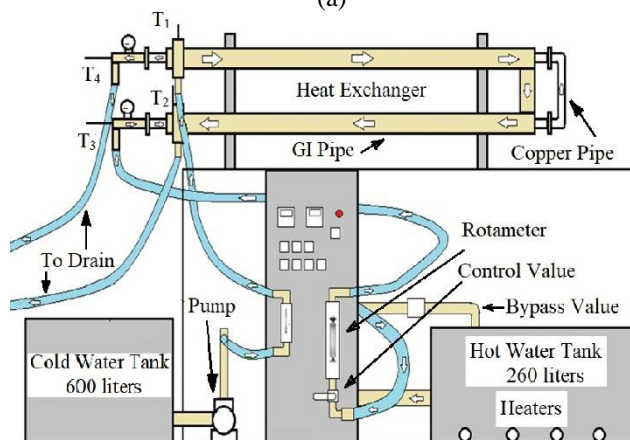
The theoretical analysis of the double pipe heat exchanger helped to develop the final size of the heat exchanger. Well before its mountings and attachments, the new apparatus underwent primary calibration. The construction of the experimental setup is made of mild steel to make the apparatus stable and sturdy. The experimental setup consists of housing for hot water tanks, cold and hot water pumps, display boards and test pipes. Two cold water tanks were used, one for the supply of fresh low-temperature cold water and the other for the storage of high-temperature cold water from the test section. Coldwater (at room temperature) and hot water (at set point $76 \pm 1^\circ\text{C}$) were allowed to flow through the annulus and inner pipe section, respectively, in the counter-flow direction. A schematic diagram of the experimental setup is shown in Fig. 2.

The test section consists of smooth inner copper tubes of 4432 mm length and outer (OD) and inner (ID) diameters of 24.5 mm and 21.5 mm respectively. The tubes were brought in, three separate parts of 2m+2m and a bend of 0.232 m. The outer G.I. pipes were selected accordingly so that there remains an effective inside diameter sufficient enough to maintain adequate flow and not to alter the original flow rate having an outer and inner diameter of 45mm and 50 mm respectively. The U-bend section is made detachable by providing flange couplings on both ends of individual lengths of copper tubes. This detachable portion was utilized to insert a full-length FST setup (when mounted on rods) easily. Two rotameters (glass tube flow meter) i.e. a cold water side small and a hot water side large were employed, with a maximum range of 100 to 1500 and 100 to 2000 LPH (liters per hour) respectively. The cold water (at room temperature) is drawn from a cold water tank (capacity of

600 liters) using a 0.5 Horsepower pump. The flow was controlled with the help of a bypass valve to set the required flow rate in a small range rotameter. For a set of readings, mass flow rates for cold & hot water were kept equal. Both flow rates (cold, hot water) start from 400 LPH and end at 1500 LPH with an increase of 100 LPH for every reading. Two pressure gauges (bourdon tube) were used of a range of $0\text{--}2 \text{ kg/cm}^2$ and a least count of 0.001 kg/cm^2 . One was installed at the entry of the test section and the other just at the exit of the test section. Four PT100 RTDs (Resistance temperature detector) sensors were used for measuring the inlet & outlet temperatures of hot (T_3, T_4) & cold water (T_1, T_2). The detailed overview of the various aspects of the experimental setup is listed in Table 1.



(a)



(b)

Figure 2. (a) Experimental setup, (b) Schematic of double pipe heat exchanger experimental setup.

Table 1. A detailed description of different components of the experimental setup.

Name	Specification	Dimension
Outer G.I. pipe	Outer Diameter	50mm
	Inner Diameter	45mm
	Length	4232mm
Inner copper pipe	Outer Diameter	24.5mm
	Inner Diameter	21.5mm
	Length	4432mm
Flat strip spring insert	Width	2.5mm
	Thickness	1mm
	Inner Diameter	21.5mm
	Length	150mm

2.2 Accretion Techniques Utilized in Current Work

An overview investigation of different types of turbulence generation devices has been conducted in a wide range of Reynolds numbers. A spring turbulator perform better for turbulent flow with conical shape and different arrangements of converging, diverging and converging and diverging. In turbulent flow, conical converging spring shows lower friction factor and disturbance to boundary layer as compared to diverging spring in circular cross-section pipe within range of 10,000 to 34,000 [10]. In contrast, the performance of helical spring tubulators inside the inner pipe of a double pipe heat exchanger. Nusselt number increases as the pitch of helical spring increases at higher Reynold number [27]. The perforated solid metal ring was tested with different open area ratio (0 to 0.0833) in the range of Reynolds numbers 6000 to 12,000. Additionally, it was noted that the friction factor decreased as the perforations increased in the metal ring inserts when liquids used as working fluid [15]. The combined performance of metal rings and twisted tape turbulaors with different pitch ratios (1 and 2) and twist ratios (2,3 and 4) was investigated and found higher heat transfer enhancement but at a cost of higher friction factors in the ranges of Reynold number from 6000 to 24000 [24]. A triple twisted tape utilised as swirl flow generator inserts with four type of twist ratio (1.92 to 6.97) under the condition of constant heat flux. As the twist ratio decreases, values of different parameter (Nu, friction factor and efficiency) increases within the range Reynold number of 7200 to 50,200 [32]. The performance of helical spring tubulators was not as good as that of conical spring tubulators. The perforated metal ring turbulators have close to half the Nusselt number values of conical spring turbulators. Single twisted tape turbulators are found to perform better in flow with a low Reynolds number as opposed to one with a higher Reynolds number because they block the flow, which results in an increased friction factor.

Compared to the other swirl inserts, Nusselt number performance of metal rings and twisted tape turbulaors was found to be the best but with higher friction factor value. Hence thermohydraulic performance of twisted tape not better at higher values of Reynold number of turbulent flow. Therefore, it may be estimated that, for double pipe heat exchanger, flat plate turbulator perform well in the turbulent flow because its having all essential benefits of conical spring, metal rings and twisted tape.

In current work, a double pipe heat exchanger is used as a standard configuration. The passive heat transfer enhancement technique was predictable in order to increase the efficiency of the current heat exchanger without affecting the surface area necessary for heat transfer. Flat strip spring turbulators as shown Fig. 3 were used as swirl generators. Diameter of FST was 21.4mm which was only adequately large enough to get fit inside the inner copper tube so that, once inside and after initiation of hot water flow any undue movement or shivering could be prohibited. FST was fabricated in Mohits springs Pvt. Ltd. located in Meerut Utter Pradesh who are specialized in the manufacturing of springs. The FSTs were visualized mounted simultaneously on thin high carbon steel at certain specific gaps known as Pitch. Rods of varying pitches were prepared to insert them in inner copper tubes. The idea behind this concept was to create an obstruction to hot water flow which consequently enhances the turbulence and swirl flow thereby augmenting the rate of heat transfer.

FSTs were mounted by brazing on high carbon steel rod to prevent any flickering when inserted in inner copper tubes and with hot water flow commenced. Several pitches were decided in advance depending upon which the brazing was done. The U bend section was detached by opening the flange couplings, and hence, the FST of $P = 15\text{cm}$ was inserted followed by 10cm and 5cm pitches.

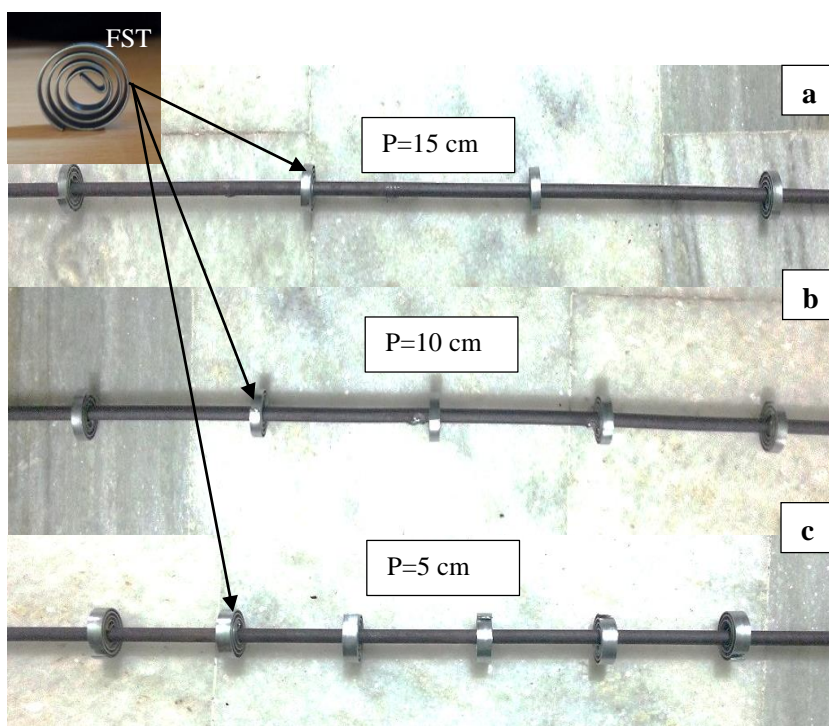


Figure 3. Flat spring tabulator (FST) mounted on rod having (a) 15 cm pitch, (b) 10cm Pitch, (c) 5cm Pitch.

3. Methodology

3.1 Problem Formulation

During the experiments, some numerical investigations constraints/assumptions were taken;

- 1) Flow is assumed to be steady, non-uniform and incompressible.
- 2) Neglecting the heat losses in all directions by maintaining isothermal condition
- 3) the inner side coefficient of thermal expansion and outer side coefficient of thermal contraction of the inner pipe in the concentric pipe of heat exchanger negates each other.
- 4) the inner surface of the pipe is assumed to be smooth.

3.2 Standardization of the Heat Exchanger Set-up

Calibration of RTD and rotameter is an important task for getting the idea of the accuracy of the experimental setup. For the calibration of RTDs, all of them were dipped (at the same depth) in a water tank maintained at a constant temperature. By taking the reference of one of the RTD (T_4) temperature readings, other RTDs reading values (T_1 to T_3) were corrected accordingly and after taking 8 number of observations, calibration found to be ± 1 . In the case of rotameter calibration, initially, two buckets (25 kg each) were used for collecting and measuring the weight of water. A flow rate of the small rotameters was varied from 300 LPH to 700 LPH. Each observation was taken for 180 seconds and

around percentage in error ranging from 1.307 to 1.774. And three observations were done for each mass flow rate of cold water rotameters. Similarly, large rotameters calibration was done by varying its mass flow rate from 800-1200 LPH for the same amount of time and observed percentage in error ranging from 1.715 to 2.614.

Before commencing the experimentation earthing of the apparatus was done. Friction factor and pressure drop readings were attained for the plane tube to verify the results with the existing standard equation for friction factor. This procedure was to eliminate the chances of deviation that could occur by repeated insertion and extraction of FSTs, which induce certain scratches (wall roughness) on the inner side of the copper tube. The readings hence obtained were compared with the Blasius equation to verify the plane tube results. This whole procedure was done at a normal temperature.

3.3 Thermal Performance Result and Repeatability

The complete experiment was re-conducted for thermal performance result and repeatability check (shown in Tables 2,3 & 4). For calculating the equivalent Reynolds number, water and pumping power was kept constant.

Table 2. Experimental data for repeatability Heat transfer versus Re for FST having pitch 15 cm.

$\dot{m}_{cw}, \dot{m}_{hw}$ (Kg/s)	T1 (°C)	T2 (°C)	T3 (°C)	T4 (°C)	Re_{hw}	Trail 1	Trail 2	%diff
						Nu_{Exp}	Nu_{Exp}	
0.113	35.9	57	75.8	57.1	9712.452	63.044	59.067	-6.732
0.141	35.8	56.2	75.8	57.9	12043.41	74.622	73.314	-1.783
0.17	35.8	55.8	75.9	58.6	14457.88	87.217	88.222	1.138
0.198	35.9	55.7	75.9	59.6	17115.7	98.551	97.270	-1.317

Table 3. Experimental data for repeatability heat transfer versus Re for FST having pitch 10 cm.

$\dot{m}_{cw}, \dot{m}_{hw}$ (Kg/s)	T1 (°C)	T2 (°C)	T3 (°C)	T4 (°C)	Re_{hw}	Trail 1	Trail 2	%diff
						Nu_{Exp}	Nu_{Exp}	
0.113	36.2	58.1	76.3	57.1	9643.40	64.32	62.770	-2.482
0.141	36.2	57.7	76.2	57.6	12043.41	78.90	77.715	-1.534
0.17	36.3	56.9	76.2	58.6	14457.88	91.31	92.489	1.269
0.198	36.3	56.7	76.1	59.6	17115.7	107.66	103.88	-3.642

Table 4. Experimental data for repeatability heat transfer versus Re for FST having pitch 5 cm.

$\dot{m}_{cw}, \dot{m}_{hw}$ (Kg/s)	T1 (°C)	T2 (°C)	T3 (°C)	T4 (°C)	Re_{hw}	Trail 1	Trail 2	%diff
						Nu_{Exp}	Nu_{Exp}	
0.113	36.3	58.7	76.9	57.1	9643.4	68.56	67.28	-1.902497
0.141	36.2	58.3	76.8	57.7	12043.41	83.18	82.11	-1.30313
0.17	36.2	57.6	76.7	58.5	14457.88	95.43	96.76	1.374535
0.198	36.4	57.2	76.5	59.3	17115.7	110.79	106.5	-4.028169

3.4 Factors Affected by Varying Pitch Between Consecutive FST

Pitch over here refers to the distance between two consecutive FST mounted on a brass rod. Apart from the enhancement in heat transfer and thermal performance installation of FST leads in the increase in pumping power requirement. The minimum pitch of the turbulators allows more turbulators on the given length which leads to more friction to the flow, more back pressure generates and all these leads to more pumping power requirement. This arrangement also separates the boundary layer commencing earlier as the pitch between two consecutive turbulators going to be decrease. Fig. 4 represents the effect of FST over variation in pitch ratio

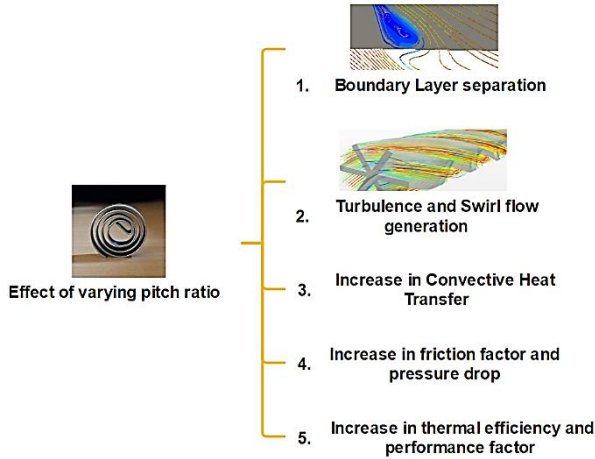


Figure 4. Repercussion by varying pitch value of FST.

4. Data Reduction

Water is taken as a working fluid for all the experiments conducted with a parametric study of the effects of variation in mass flow rate for turbulent case. Installation of FST with varying pitch ratio influences the flow conditions including an adverse effect i.e. increment of friction factor. Different equations required for the basis of such experiments are summed as follows:

Quantity of heat flow [33] for hot and cold water loops can be calculated from Eqn. (1) and (2)

$$\dot{Q}_c = \dot{m}_c \times C_{pc} \times (T_{ce} - T_{ci}) \quad (1)$$

$$\dot{Q}_h = \dot{m}_h \times c_{ph} \times (T_{hi} - T_{he}) \quad (2)$$

The arithmetic average of heat exchange from the hotter and colder fluid streams is

$$Q_{ave.} = \frac{Q_h + Q_c}{2} \quad (3)$$

The overall heat transfer coefficient can be calculated as

$$U = \frac{Q_{ave.}}{A \times l m t d} \quad (4)$$

$$l m t d = \frac{(T_{hi} - T_{ce}) - (T_{he} - T_{ci})}{\ln \left(\frac{T_{hi} - T_{ce}}{T_{he} - T_{ci}} \right)} \quad (5)$$

Where A is the circumferential area of the inner pipe.

4.1 Standard Equation

The non-dimensional numbers; Nu, Re and Pr calculated from Eqn:

$$Nu = \frac{hD}{k} \quad (6)$$

$$Re = \frac{\rho V D}{\mu} \quad (7)$$

$$Pr = \frac{\mu c_p}{k} \quad (8)$$

$$\lambda = \frac{\Delta P}{\left(\frac{l}{d} \right) \left(\frac{\rho V^2}{2} \right)} \quad (9)$$

$$V = \frac{\dot{m}}{\rho A_c} \quad (10)$$

4.2 Heat Transfer and Friction Factor Calculation

For the heat transfer calculations, some standard equations from the literatures were used for the experimental flow conditions.

DittusBoelter Equation [34]

$$Nu = 0.023 Re^{0.8} Pr^{0.3} \quad (11)$$

Friction factor for the different flow arrangements were calculated from Blasius Equation and Darcy-weisbach equations [33]

$$\lambda = \frac{0.3164}{Re^{0.25}} \quad (12)$$

$$\lambda = \frac{\Delta P}{\frac{L}{D} \frac{\rho V^2}{2}} \quad (13)$$

Thermal performance factor calculation at constant pumping power

$$\left(\lambda Re^3 \right)_{PT} = \left(\lambda Re^3 \right)_T \quad (14)$$

The thermal performance factor and performance evaluation criteria is the key parameter in designing effective heat exchanging devices [35]. The thermal performance factor (η) is the ratio of the Nusselt number ratio (Nu_T/Nu_{PT}) to the friction factor ratio (λ_T/λ_{PT}) considering constant pumping power and can be represented as

$$\eta = \frac{Nu_T / Nu_{PT}}{\left(\lambda_T / \lambda_{PT} \right)^{1/3}} \quad (15)$$

4.3 Uncertainty Calculation

Mass flow rate, pressure (at inlet and exit), and temperature distribution were the variables measured by the test rig. Before being used in the experimental setting, all variable measuring equipment were calibrated. The two crucial factors, Nusselt number and Reynolds number, were going to be used to understand the experiment's measured variables. Temperature and pressure drop are the most effect-causing variables for Nusselt number, while flow rate is the greatest effect-causing variable for Reynold number. Fluid thermo-physical properties, on the other hand, had a significant impact on both of them.

The root sum square equation, which combines the effects of each distinct input as proposed by Kline and McClintock [36], could be used to determine the uncertainties in the computed findings with improved precision. The uncertainties in the aforementioned equations are caused by inaccuracies in the primary parameters, as indicated in Table 5. The highest computed uncertainty in heat transfer coefficient, Prandtl number, and friction factor obtained from all experiments are 4%, 2.5%, and 5%, respectively. The computed uncertainty in the results is calculated from Eq. 16.

$$R = \pm \sqrt{\left(\frac{\delta R}{\delta x_1} \delta x_1\right)^2 + \left(\frac{\delta R}{\delta x_2} \delta x_2\right)^2 + \dots + \left(\frac{\delta R}{\delta x_n} \delta x_n\right)^2} \quad (16)$$

Where δx is the uncertainty of the independent individual variables and $\frac{\partial R}{\partial x}$ is sensitivity.

Table 5. Uncertainties in the main parameters.

Parameter	Uncertainty (%)
Annulus-side Reynolds number	± 1.77**
Tube-side Reynolds number	± 2.61**
Thermocouple	± 0.1 °C*
Pressure transducer	± 0.35*
Heating wire	± 0.15*

* Based on manufacturer claim.

** Based on calibration.

4.4 Preparation of Wilson Chart and Standard Equations

The calculation of the film heat transfer [37], [38] can be estimated by the very popular technique known as the Wilson plot. This plot is based on the overall thermal resistance in the total heat transfer in the form of convection. For all sets of experiment, except the first term, all other resistance is constant on the RHS of Eq. 17.

$$\frac{1}{U_i} = \frac{1}{h_i} + \frac{h_i}{d_o h_o} + \frac{x_w d_i}{k_w d_i} \quad (17)$$

As a flow on inner waterside is turbulent and the variation in thermal properties are negligible, for a smooth tube with a flow rate of more than 10000 Reynold number, the Seider Tate equation is of the form

$$h_i = A Re^{0.8} \quad (18)$$

Therefore, from Eq. 17 and Eq. 18, it can be written as

$$\frac{1}{U_i} = \frac{1}{A Re^{0.8}} + K \quad (19)$$

Here, K is a constant and its value is to be estimated on the intercept of the y-axis of the Wilson chart ($1/U_i$ vs. $1/Re^{0.8}$). This value was put in Eq. 17 to obtain the value of h_i . This expression is in the form of the exponent of Reynold number.

The same procedure as was done for the plane tube was repeated for whole pitches of FST. Heat transfer results were obtained by preparing Wilson Charts between Reynolds number (Re) and overall heat transfer coefficient (U) it can be seen in section 5.3.

5. Result and Discussion

In this analysis effect of Flat Strip Spring Turbulator (FST) installed inside the double pipe heat exchanger in the counter-current flow arrangement was analysed. Friction factor increment means a decrease in the pitch ratio of turbulators used in the experiment, which ultimately affects the pressure drop i.e. pumping power. But, for maintaining higher value of Reynolds number, a constant (high) pumping power is required. Hence, it is desired to maintain an optimum condition i.e. balance between pitch ratio, friction factor, pressure loss, and ultimately in pumping power. The main function of a turbulator is to generate detachment and reattachment of flow around them and as a result of this, reduces the effect of the boundary layer (when heat is transferred through the laminar effect). This separation of flow generates proper mixing regions (with large turbulence energy) which ultimately destroy the eddies and vortex formation for heat transfer enhancement.

5.1 Plain Tube Experimentation

For hot water, heaters were used to heat the water to 76°C, as this temperature lied within the limits of the heating capacity of heaters and could be easily maintained in the working conditions. A temperature regulator is used for maintaining constant temperature. The tank is connected to pump (centrifugal type) for circulation of hot water inside the inner pipe of the heat exchanger and for controlling the flow rate a bypass valve is used (recirculation the hot water back into the tank). This hot water allowed to pass through the inner tube of heat exchanger at a desired mass flow rate and simultaneously cold water flow was initiated and this set up was left continued for at least 20 minutes to attain a steady-state condition. Now that a steady state was achieved, the main experimentation was commenced by adjusting the mass flow rates by using rotameters of both cold water and hot water side at desired values. The readings from RTDs were obtained only when a steady condition is achieved. This procedure was repeated at various flow rates (0.1134-0.425 Kg/s) of cold and hot water. Under the assumption of uniform heat flux, the calculation of Nusselt numbers is done and compared with the fundamental Eqn. 11 (provided by Dittus and Boelter) for validating the current plane tube.

The Nusselt number variation with Reynolds number for plain tube experiment are shown in the Fig.5(a).Whereas, it was noted that the variation of Nusselt number within the acceptable range of Dittus– Boelter equation correlation [34]. Before beginning any heat exchanger related experiment utilizing turbulator, measurement of friction factor as a secondary parameter is necessary. So, verifying (under similar test conditions) the current plain inner copper tube for the friction factor parameter by comparing of the current data obtained with those obtained from the Blasius correlation. This variation of friction factor with the Blasius equation is show in Fig.5(b).

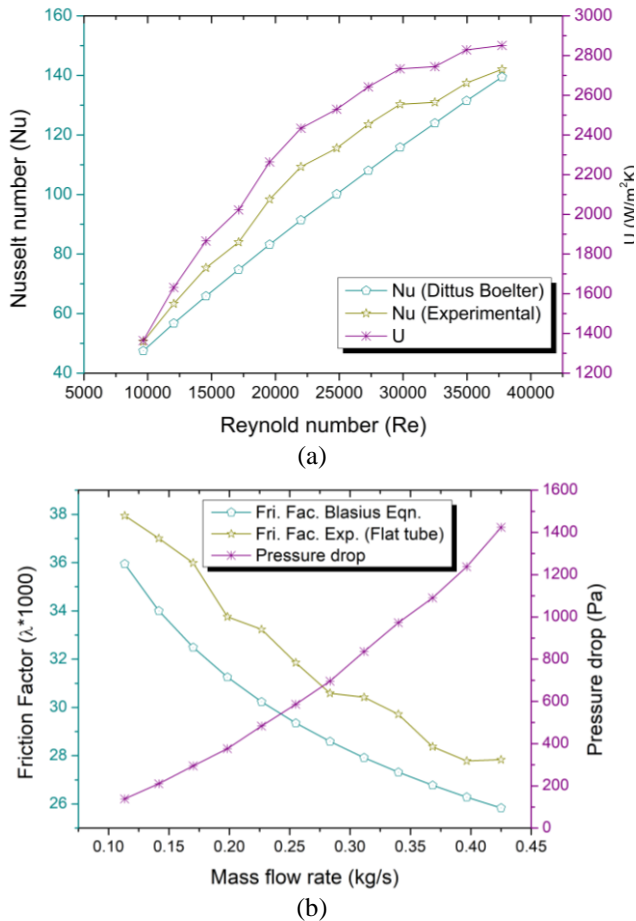


Figure 5. (a) Nusselt number and overall heat transfer coefficient for plane tube, (b) Variation in friction factor and pressure drop for plane tube.

5.2 Effect of FST Turbulator on Nusselt Number

Effect on tubes with FST at different pitches (PR=15, 10, and 5cm) on the heat transfer rate (Nu) is demonstrated in Fig. 6. For all values of Reynolds number, the heat transfer rate for FST is higher than those of the plain tube and this is due to the destruction of the thermal boundary layer present near the inner tube wall. In different turbulator arrangements, it is found that with the decrease of pitch the heat transfer rate increases. This is because since, FST with a smaller PR of 5cm, create more intervention in the generation of thermal as well as hydrodynamic boundary layer with a greater degree of turbulence than that of higher PR of 15cm. The quantitative analysis reveals that the percentage heat transfer rate in the tube with FST of P =15cm, P=10cm, P= 5cm is 7.93%, 13.09%, and 14.26% higher than those in the plain tube at Re =17115.70.

Fig. 6. (b) Indicate the Nusselt number ratio variation with respect to Reynolds number. From the graph, it is evident that Nusselt number values decrease with increasing Reynolds number or its having higher rate of heat transfer at lower values of Reynolds number. This occurs primarily because at low Reynolds numbers the thermal boundary layer thickness is higher near the surface of the pipe, limiting heat transfer, while after putting the FST in place, the boundary layer effect is no longer noticeable. It is evident that, 10 cm pitch FST has a higher value of Nusselt number ratio as compared to 15cm pitch. In all three cases, the values attained were greater than unity, demonstrating the advantage of using FST as an insert in heat exchangers as compared to a plan tube. It is found that the highest and

lowest values of the Nusselt number ratio are in between 1.20 and 1.13 for FSTs with a pitch of 5 cm, whereas in case of pitch 15 cm it is between 1.10 and 1.05 for FSTs.

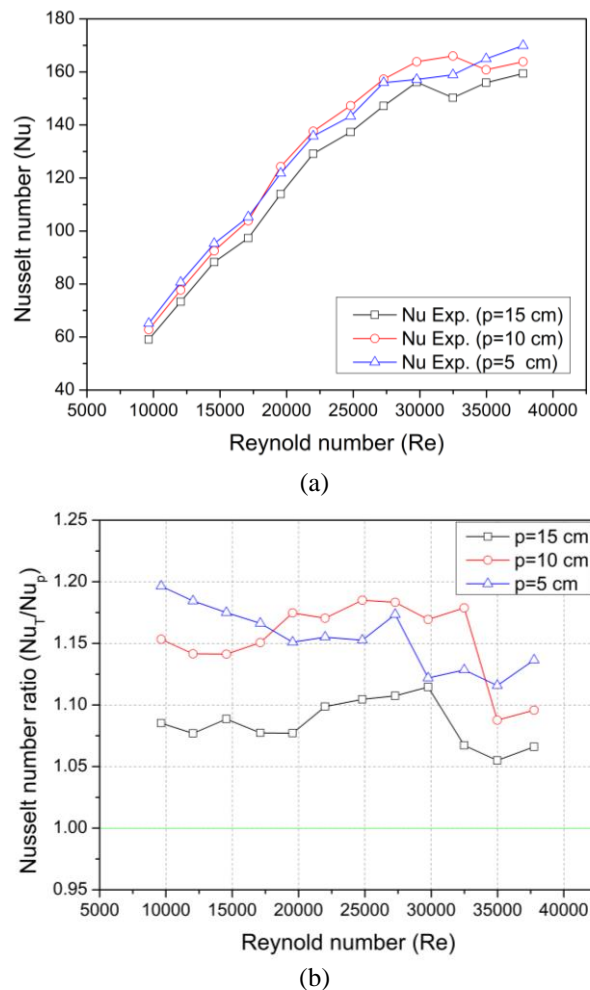
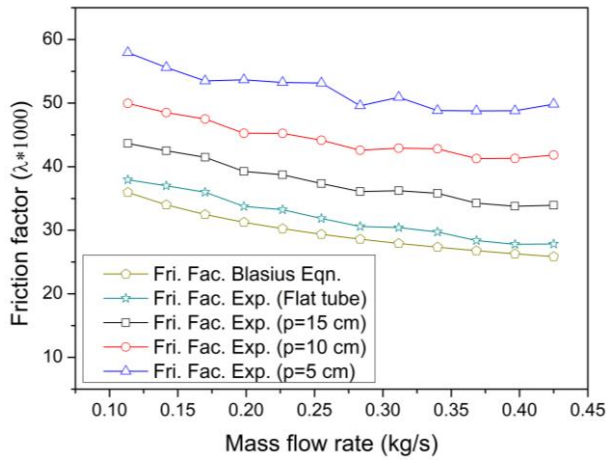


Figure 6. (a) Heat transfer enhancement by FST, (b) Effect of pitch values on Nusselt number.

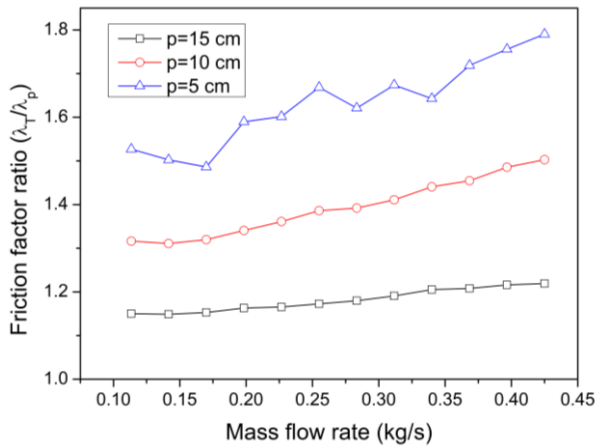
5.3 Effect of FST Turbulator on Friction Factor

The friction factor is one of the important parameters for improving the thermal performance factor in heat exchangers. Across the test section, friction factor value varies directly with the pressure drop values and inversely with the square of fluid velocity values. Whereas, by considering Reynolds number increment, friction factor decreases but pressure drop increases. So, as the turbulator used in the heat exchanger, the friction factor will increase because of the obstruction in the flow. Therefore, it is very important to find out a turbulator that imparted the lowest friction factor.

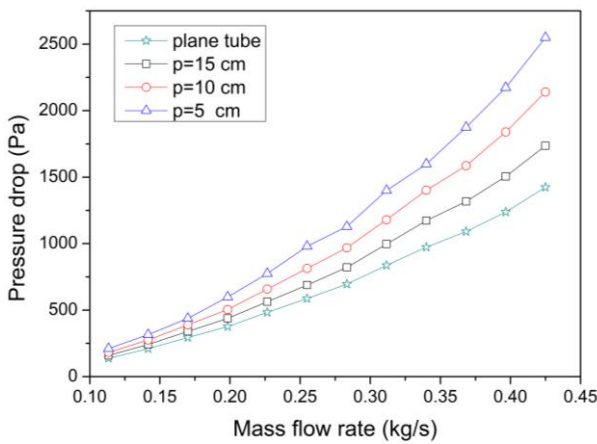
From the scenario of Fig. 7 (a&b), It is concluded that the value of friction factor increases as the pitch ratio decreases for the same Reynolds number. The reason behind this trend is smaller the distance between FSTs, and more obstructions faced by the flow which ultimately causes an increase in friction factor. The simple fact is that, when the distance between two consecutive FSTs is less, more space is available for mounting the FSTs on the cylindrical rod inside the inner copper tube, thus the more obstruction against the flow stream of hot water. Hence, more turbulence results in a high-pressure drop.



(a)



(b)



(c)

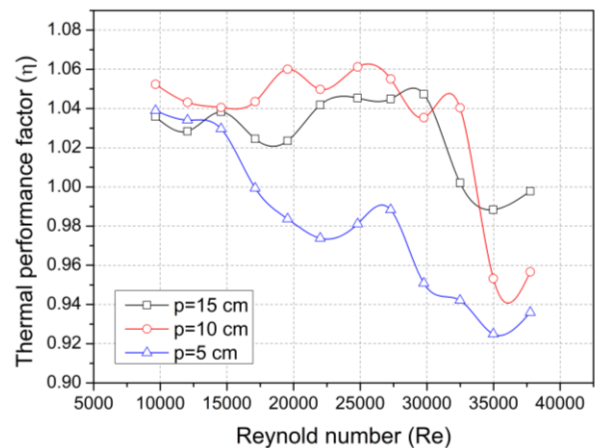
Figure 7. (a) Influence of different pitch value on (a-b) turbulator on friction factor, (c) Pressure drop.

The turbulator acts as an obstruction, as the difference between two consecutive FST increases, local flow velocity quantity also increases (which means local Reynolds number increase). The occurrence of these events may generate lots of vortices and these vortices when faces centrifugal force due to secondary flows cause pressure drop as compare to plan tube. As shown in Fig. 7(c) that as the FST pitch decreases pressure drop increases for the constant value of the Reynolds number. FST pitch increment means that obstruction located at larger distances and as a result of this decrement in Reynolds number and generation of vortices is observed with an increment in hydraulic diameter. All these phenomena together cause the decrement in pressure drop.

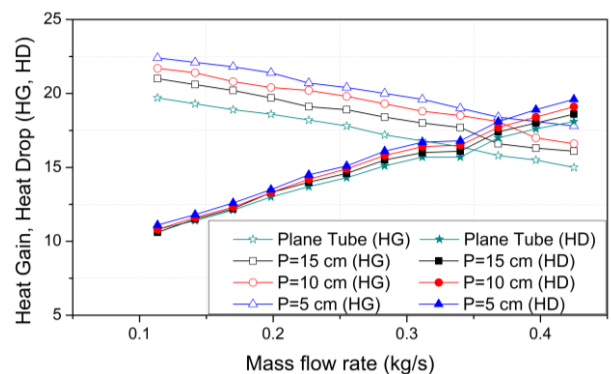
5.4 Effect of FST Turbulator on the Thermal Performance Factor

Only thermal aspects cannot be set as the final criteria for the selection of FST. Here, an optimal value of pitch should be selected which has better heat transport capability and also have a lower value of frictional loss (pumping power). The thermal performance factor is also one of the important factors to count both the effect in the heat exchanger. A significant increment in Nusselt number and friction factor is always observed for various types of turbulators. So, designing the geometry of turbulator is an important task with a view of obtaining maximum thermal performance factors. As can be seen in Fig. 8(a) at constant pumping power, it is evident from the graph that Reynold number and thermal performance factor are in inverse relation with each other. Also, this can be concluded that because of improved thermal and hydraulic performance, the FSTs at $P = 10$ cm (having the same pumping power) are most efficient.

As can be seen from Fig. 8(b) there occur a significant change in heat gain and heat drop trends at different mass flow rate. It was observed that at higher mass flow rate heat drop and heat gain become approximately equal and the general trend was the heat drop rate decreases with increase in mass flow rate and rate of heat gain increases with increase in mass flow rate.



(a)



(b)

Figure 8. (a) Variation in thermal performance factor with Reynold number, (b) HT characteristics at constant \dot{m}_{hw} & \dot{m}_{cw} .

5.5 Experimental Results Conjugated to Wilson Plot

Wilson plot is a very important tool that is utilized to check the performance of different types of heat exchangers [42]. Through this approach, the overall heat transfer coefficient value can directly be calculated which is not

easier indirect calculation from the experimental results due to inaccessible surface temperature values. The experimental results obtained from the experiment on double pipe heat exchanger experimental setup with flat strip spring Turbulator insert were analyzed with Wilson chart (having variation between overall heat transfer coefficient (U) and Reynold number). The results were plotted between $10000/U_i$ and $10000/Re^{0.8}$, which is presented in Fig. 9. The variation of $10000/U$ follows the linear trend as of the Wilson plot. However, the experimental values are slightly lesser than that of the straight-line of the Wilson plot.

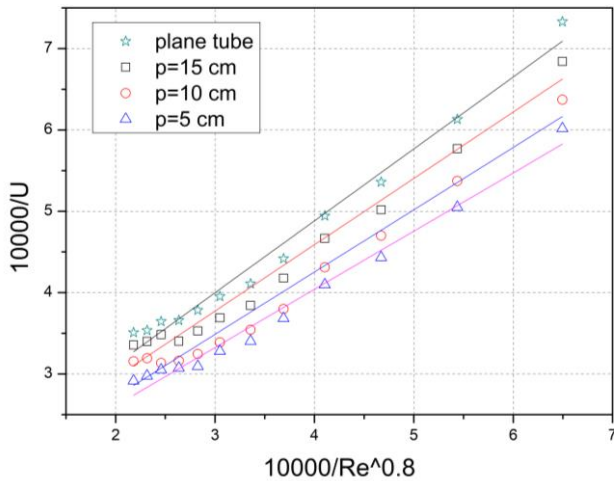


Figure 9. Visualization of overall heat transfer coefficient with Wilson plot.

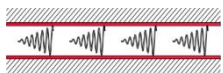





5.6 Comparison of Performance Parameters of Different Turbulators

In the Table 6, the term “Nusselt number ratio” (Nu_{max}/Nu_p) is the ratio of maximum Nusselt number after augmentation to Nusselt number of the plane tube, and “friction factor ratio” (λ_{max}/λ_p) is the ratio of maximum friction factor after augmentation to friction factor of the plan tube. In current work, the Nusselt number ratio comes only 1.2 at the expense of friction factor ratio of 1.44 in a range of Reynolds no. (9000–38,000). Whereas, maximum increment in Nusselt number ratio is claimed by Singh et. al. [24] i.e. 4.6 but at a higher value of friction factor ratio of 36.07 in a range of Reynolds no. (6300– 22500) and as it is well known that, with the increment in Reynolds number friction factor also increases which further increases required pumping power and makes the heat exchange process uneconomical. So, in the present study even at a higher value of Reynolds number friction factor obtaining well-accepted range as compared to the previous studies.

6. Conclusion

The present experimental study presents the potential application of FST to enhance the heat transport performance of a concentric double tube heat exchanger. The experimental objectives investigation was successfully carried out with the insertion of FST at various pitch values at varying cold and hot water flow rate of 500 to 1500 LPH and 500 to 2000 LPH, respectively. All the time, the experiment was in turbulent flow with Reynold number ranging from 9000 to 38000, which significantly influences the different parameter of heat exchanger (Nusselt number, friction, and thermal performance factor). The most remarkable conclusions drawn after conducting this experiment are:

Table 6. Comparison of performance parameters of different turbulators.

Author	Turbulator used	Parameters	Reynolds Number	Nusselt Number ratio	Friction factor ratio	Image
Karakaya et. al. [10]	Conical spring turbulators	different cone angle (30°, 45°, 60°)	10,000 to 34,000	$Nu_{max} \approx 3.33 Nu_p$	$\lambda_{max} \approx 1.72 \lambda_p$	
Sheikholeslami et. al. [15]	typical and perforated circular turbulators	open area ratio (0 to 0.0625), pitch ratio (1.83 to 5.83)	6000 to 12,000	$Nu_{max} \approx 2.12 Nu_p$	$\lambda_{max} \approx 11.40 \lambda_p$	
Singh et. al. [24]	solid ring tubular (SRT) with Number of twisted tapes (TT): 1, 2, 3, 4	Pitch ratios (1 and 2, twist ratios (2, 3, and 4)	6300 to 22500	$Nu_{max} \approx 4.6 Nu_p$	$\lambda_{max} \approx 36.07 \lambda_p$	
Akpinar[27]	helical (spring shaped)		6500 to 13,000	$Nu_{max} \approx 2.64 Nu_p$	$\lambda_{max} \approx 2.74 \lambda_p$	
Bhuiya et al. [39]	Triple twisted tape	Twist ratio- 1.92–6.79	7200 to 50,200	$Nu_{max} \approx 3.85 Nu_p$	$\lambda_{max} \approx 4.2 \lambda_p$	
Present study	Flat strip spring turbulator	At different pitch ratio of 5, 10 & 15	9000 to 38000	$Nu_{max} \approx 1.2 Nu_p$	$\lambda_{max} \approx 1.44 \lambda_p$	

- The enhancement of heat transfers with flat spring inserts of P =15cm, P=10cm, P= 5cm is 7.93%, 13.09%, and 14.26% higher than those in the plain tube at Re =17115.69 and flow rates at 0.19839 kg/s. Over the range investigated, the maximum heat transfer rise was about 20% for FST at pitch 5cm.
- The heat transfer rate and friction factor of FSTs increase with decreasing pitch due to the number FSTs present on the cylindrical rod was high inserted in the copper tube. However, the thermal performance factor increases with decreasing pitch
- The friction factor obtained from using the PCR with pitch 15, 10, and 5cm are found to be respectively, 17%, 30%, and 39%, over the plain tube at Reynolds number of 17997.71. An increase in the pitch of FSTs causes a reduction in Nusselt numbers as well as friction factors. The maximum friction factor rise was about 44% for Reynolds number of 22497.1.
- The maximum heat gain & heat drop-in plan tube is 19.7 & 18.1. On 15cm pitch, Maximum heat gain& heat drop is 21 & 18.6. On 10cm pitch, Maximum heat gain & heat drop was 21.7 & 19.1. On 5cm pitch, Maximum heat gain & heat drop is 22.4 & 19.6.

As the pitch between two consecutive FSTs decreases not only heat transfer rate increase but also an adverse effect increases i.e. friction factor. An optimal pitch value is suggested from this study because increasing the turbulator is not only the solution for heat transfer enhancement, a downside of this arrangement is the increasing pressure drop which leads to more power requirement and this should be considered for optimization to the maximum performance of heat exchanger.

Nomenclature

L	Total length of pipe
D	Hydraulic diameter
V	Velocity of water
ΔP	Frictional pressure drop
c	Specific heat
d	Diameter of inner pipe
Nu	Nusselt Number
Re	Reynold Number
P	Pitch
\dot{m}	Mass flow rate
c	Specific heat
T	Turbultor
A	Area
PT	Plane Tube
λ	Friction factor
ρ	Density of fluid
η	Thermal performance factor
LMTD	Log Mean Temperature Difference
RTD	Resistance temperature detector
HG	Heat Gain
HD	Heat Drop

Subscript

i	Inner
o	Outer
c	Cross sectional
max	Maximum

References:

- [1] A. E. Bergles, R. L. Bunn, and G. H. Junkhan, "Extended performance evaluation criteria for enhanced heat transfer surfaces," *Letters in Heat and Mass Transfer*, vol. 1, no. 2, pp. 113–120, Nov. 1974, doi: 10.1016/0094-4548(74)90147-7.
- [2] W. M. Rohsenow, J. P. Hartnett, E. N. Ganic, and P. D. Richardson, *Handbook of Heat Transfer Fundamentals (Second Edition)*, vol. 53, no. 1. 1986.
- [3] D. B. Berkowitz, *Handbook on Syntheses of Amino Acids: General Routes for the Syntheses of Amino Acids*, vol. 132, no. 50. 2010.
- [4] H. S. Dizaji and S. Jafarmadar, "Experiments on New Arrangements of Convex and Concave Corrugated Tubes through a Double-pipe Heat Exchanger," *Experimental Heat Transfer*, vol. 29, no. 5, pp. 577–592, Sep. 2016, doi: 10.1080/08916152.2015.1046015.
- [5] H. M. Şahin, E. Baysal, and A. R. Dal, "Experimental and numerical investigation of thermal characteristics of a novel concentric type tube heat exchanger with turbulators," *International Journal of Energy Research*, vol. 37, no. 9, pp. 1088–1102, Jul. 2013, doi: 10.1002/er.2919.
- [6] J. K. Dasmahapatra and M. R. Rao, "Laminar flow heat transfer to generalised power law fluids inside circular tubes fitted with regularly spaced twisted tape elements for uniform wall temperature condition," in *American Society of Mechanical Engineers, Heat Transfer Division, (Publication) HTD*, 1991, vol. 174, pp. 51–58.
- [7] S. Al-Fahed and W. Chakroun, "Effect of tube-tape clearance on heat transfer for fully developed turbulent flow in a horizontal isothermal tube," *International Journal of Heat and Fluid Flow*, vol. 17, no. 2, pp. 173–178, Apr. 1996, doi: 10.1016/0142-727X(95)00096-9.
- [8] R. M. Manglik and A. E. Bergles, "Heat transfer enhancement and pressure drop in viscous liquid flows in isothermal tubes with twisted-tape inserts," *Wärme- und Stoffübertragung*, vol. 27, no. 4, pp. 249–257, Apr. 1992, doi: 10.1007/BF01589923.
- [9] P. Zamankhan, "Heat transfer in counterflow heat exchangers with helical turbulators," *Communications in Nonlinear Science and Numerical Simulation*, vol. 15, no. 10, pp. 2894–2907, Oct. 2010, doi: 10.1016/j.cnsns.2009.10.025.
- [10] H. Karakaya and A. Durmuş, "Heat transfer and exergy loss in conical spring turbulators," *International Journal of Heat and Mass Transfer*, vol. 60, no. 1, pp. 756–762, May 2013, doi: 10.1016/j.ijheatmasstransfer.2013.01.054.
- [11] D. Yadav, Z. Upadhyay, A. Kushwaha, and A. Mishra, "Analysis Over Trio-Tube with Dual Thermal Communication Surface Heat Exchanger [T.T.H.Xr.]," in *Lecture Notes in Mechanical Engineering*, 2020, pp. 1–13.
- [12] D. Yadav, A. Kushwaha, and A. Mishra, "Design and Fabrication of Trio Tube Heat Exchanger Experimental Setup," *SSRN Electronic Journal*, 2020, doi: 10.2139/ssrn.3576468.

- [13] M. Sheikholeslami and D. D. D. Ganji, "Heat transfer enhancement in an air to water heat exchanger with discontinuous helical turbulators; experimental and numerical studies," *Energy*, vol. 116, pp. 341–352, Dec. 2016, doi: 10.1016/j.energy.2016.09.120.
- [14] M. Sheikholeslami, M. Gorji-Bandpy, and D. D. D. Ganji, "Effect of discontinuous helical turbulators on heat transfer characteristics of double pipe water to air heat exchanger," *Energy Conversion and Management*, vol. 118, pp. 75–87, Jun. 2016, doi: 10.1016/j.enconman.2016.03.080.
- [15] M. Sheikholeslami and D. D. D. Ganji, "Heat transfer improvement in a double pipe heat exchanger by means of perforated turbulators," *Energy Conversion and Management*, vol. 127, pp. 112–123, Nov. 2016, doi: 10.1016/j.enconman.2016.08.090.
- [16] K. Nanan, C. Thianpong, M. Pimsarn, V. Chuwattanakul, and S. Eiamsa-ard, "Flow and thermal mechanisms in a heat exchanger tube inserted with twisted cross-baffle turbulators," *Applied Thermal Engineering*, vol. 114, pp. 130–147, Mar. 2017, doi: 10.1016/j.applthermaleng.2016.11.153.
- [17] N. Mashoofi, S. M. Pesteei, A. Moosavi, and H. Sadighi Dizaji, "Fabrication method and thermal-frictional behavior of a tube-in-tube helically coiled heat exchanger which contains turbulator," *Applied Thermal Engineering*, vol. 111, pp. 1008–1015, Jan. 2017, doi: 10.1016/j.applthermaleng.2016.09.163.
- [18] D. Panahi *et al.*, "Heat transfer enhancement of shell-and-coiled tube heat exchanger utilizing helical wire turbulator," *Applied Thermal Engineering*, vol. 115, no. 2–3, pp. 607–615, Mar. 2017, doi: 10.1016/j.applthermaleng.2016.12.128.
- [19] S. P. Nalavade, C. L. Prabhune, and N. K. Sane, "Effect of novel flow divider type turbulators on fluid flow and heat transfer," *Thermal Science and Engineering Progress*, vol. 9, pp. 322–331, Mar. 2019, doi: 10.1016/j.tsep.2018.12.004.
- [20] S. Khorasani, S. Jafarmadar, S. Pourhedayat, M. A. A. Abdollahi, and A. Heydarpour, "Experimental investigations on the effect of geometrical properties of helical wire turbulators on thermal performance of a helically coiled tube," *Applied Thermal Engineering*, vol. 147, pp. 983–990, Jan. 2019, doi: 10.1016/j.applthermaleng.2018.09.092.
- [21] A. E. Zohir, M. A. Habib, and M. A. Nemitallah, "Heat Transfer Characteristics in a Double-Pipe Heat Exchanger Equipped with Coiled Circular Wires," *Experimental Heat Transfer*, vol. 28, no. 6, pp. 531–545, Nov. 2015, doi: 10.1080/08916152.2014.915271.
- [22] N. Budak, H. L. Yucel, and Z. Argunhan, "Experimental and Numerical Investigation of the Effect of Turbulator on Heat Transfer in a Concentric-type Heat Exchanger," *Experimental Heat Transfer*, vol. 29, no. 3, pp. 322–336, May 2016, doi: 10.1080/08916152.2014.976723.
- [23] A. Kumar, S. Chamoli, M. Kumar, and S. Singh, "Experimental investigation on thermal performance and fluid flow characteristics in circular cylindrical tube with circular perforated ring inserts," *Experimental Thermal and Fluid Science*, vol. 79, pp. 168–174, Dec. 2016, doi: 10.1016/j.expthermflusci.2016.07.002.
- [24] V. Singh, S. Chamoli, M. Kumar, and A. Kumar, "Heat transfer and fluid flow characteristics of heat exchanger tube with multiple twisted tapes and solid rings inserts," *Chemical Engineering and Processing: Process Intensification*, vol. 102, pp. 156–168, Apr. 2016, doi: 10.1016/j.cep.2016.01.013.
- [25] A. Kumar, S. Singh, S. Chamoli, and M. Kumar, "Experimental Investigation on Thermo-Hydraulic Performance of Heat Exchanger Tube with Solid and Perforated Circular Disk Along with Twisted Tape Insert," *Heat Transfer Engineering*, vol. 40, no. 8, pp. 616–626, May 2019, doi: 10.1080/01457632.2018.1436618.
- [26] R. Datt, M. S. Bhist, A. D. Kothiyal, R. Maithani, and A. Kumar, "Effect of square wing with combined solid ring twisted tape inserts on heat transfer and fluid flow of a circular tube heat exchanger," *International Journal of Green Energy*, vol. 15, no. 12, pp. 663–680, Sep. 2018, doi: 10.1080/15435075.2018.1525552.
- [27] E. K. Akpınar, "Evaluation of heat transfer and exergy loss in a concentric double pipe exchanger equipped with helical wires," *Energy Conversion and Management*, vol. 47, no. 18–19, pp. 3473–3486, Nov. 2006, doi: 10.1016/j.enconman.2005.12.014.
- [28] C. Maradiya, J. Vadher, and R. Agarwal, "The heat transfer enhancement techniques and their Thermal Performance Factor," *Beni-Suef University Journal of Basic and Applied Sciences*, vol. 7, no. 1, pp. 1–21, Mar. 2018, doi: 10.1016/j.bjbas.2017.10.001.
- [29] M. Sheikholeslami, M. Gorji-Bandpy, and D. D. Ganji, "Review of heat transfer enhancement methods: Focus on passive methods using swirl flow devices," *Renewable and Sustainable Energy Reviews*, vol. 49, pp. 444–469, Sep. 2015, doi: 10.1016/j.rser.2015.04.113.
- [30] M. Omid, M. Farhadi, and M. Jafari, "A comprehensive review on double pipe heat exchangers," *Applied Thermal Engineering*, vol. 110, pp. 1075–1090, Jan. 2017, doi: 10.1016/j.applthermaleng.2016.09.027.
- [31] H. Li *et al.*, "A comprehensive review of heat transfer enhancement and flow characteristics in the concentric pipe heat exchanger," *Powder Technology*, vol. 397, p. 117037, Jan. 2022, doi: 10.1016/j.powtec.2021.117037.
- [32] M. M. K. Bhuiya, M. S. U. Chowdhury, M. Shahabuddin, M. Saha, and L. A. Memon, "Thermal characteristics in a heat exchanger tube fitted with triple twisted tape inserts," *International Communications in Heat and Mass Transfer*, vol. 48, pp. 124–132, Nov. 2013, doi: 10.1016/j.icheatmasstransfer.2013.08.024.
- [33] C. Ringsted, K. Eliassen, I. H. Gøthgen, and O. Siggaard-Andersen, "Positive correlation between 'the arterial oxygen extraction tension' and mixed venous po2 but lack of correlation between 'the oxygen compensation factor' and cardiac output in 38 patients," vol. 50, no. S203, 1990.
- [34] F. W. Dittus and L. M. K. Boelter, "Heat transfer in automobile radiators of the tubular type," *International Communications in Heat and Mass Transfer*, vol. 12, no.

- 1, pp. 3–22, 1985, doi: 10.1016/0735-1933(85)90003-X.
- [35]R. L. Webb, “Performance evaluation criteria for use of enhanced heat transfer surfaces in heat exchanger design,” *International Journal of Heat and Mass Transfer*, vol. 24, no. 4, pp. 715–726, Apr. 1981, doi: 10.1016/0017-9310(81)90015-6.
- [36]S. Kline and F. McClintock, “Describing uncertainties in single-sample experiments,” *Mechanical Engineering*, vol. 75, pp. 3–8, 1953.
- [37]D. Wilkie, “Wilson Plot,” in *A-to-Z Guide to Thermodynamics, Heat and Mass Transfer, and Fluids Engineering*, Begellhouse, 2011.
- [38]J. Fernández-Seara, F. J. Uhía, J. Sieres, and A. Campo, “Experimental apparatus for measuring heat transfer coefficients by the Wilson plot method,” *European Journal of Physics*, vol. 26, no. 3, pp. N1–N11, May 2005, doi: 10.1088/0143-0807/26/3/N01.
- [39]M. M. Bhunia, K. Panigrahi, S. Das, K. K. Chattopadhyay, and P. Chattopadhyay, “Amorphous graphene – Transformer oil nanofluids with superior thermal and insulating properties,” *Carbon*, vol. 139, pp. 1010–1019, Nov. 2018, doi: 10.1016/j.carbon.2018.08.012.